

## Supplementary Information for

### **Lineage tracing and targeting of IL17RB<sup>+</sup> tuft cell-like human colorectal cancer stem cells**

Norihiro Goto, Akihisa Fukuda, Yuichi Yamaga, Takaaki Yoshikawa, Takahisa Maruno, Hisatsugu Maekawa, Susumu Inamoto, Kenji Kawada, Yoshiharu Sakai, Hiroyuki Miyoshi, Makoto Mark Taketo, Tsutomu Chiba, Hiroshi Seno

Corresponding Author: Hiroshi Seno  
e-mail: [seno@kuhp.kyoto-u.ac.jp](mailto:seno@kuhp.kyoto-u.ac.jp)

#### **This PDF file includes:**

Supplementary text  
Figs. S1 to S14  
Tables S1  
Captions for movies S1  
References for SI reference citations

#### **Other supplementary materials for this manuscript include the following:**

Movies S1

## SI Appendix, Materials and Methods

### Animal models

*Il17rb-CreERT2-IRES-EGFP* mice were generated by homologous recombination in embryonic stem cells targeting the CreERT2-IRES-EGFP cassette to the first ATG codon of *Il17rb* locus, as illustrated in Supplementary Figure 1. *Lgr5-EGFP-IRES-CreERT2* mice (JAX strain 008875), *Apc<sup>Min</sup>* mice (JAX strain 002020), and *Rosa26 tdTomato* mice (JAX strain 007914) were obtained from The Jackson Laboratory. *Dclk1-CreERT2-IRES-EGFP* mice and *Ctnnb1<sup>lox(ex3)</sup>* mice were generated as described previously (1, 2). These mice were maintained in a C57BL/6 background. BALB/cAJcl-*nu/nu* mice and NODShiJic-*scid* mice were obtained from CLEA Japan. For induction of Cre-mediated recombination, 100  $\mu$ L of 20 mg/mL tamoxifen (Sigma-Aldrich, St. Louis, MO) in corn oil twice a day over 2 consecutive days or once a day over 3 consecutive days was intraperitoneally injected. For long-term *in vivo* ablation experiments, 50  $\mu$ g of dimerizer (AP20187, Takara, Shiga, Japan) and 1 mg tamoxifen were administered alternately every other days.

### Organoid/spheroid culture

Organoid/spheroid cultures were established from murine intestinal tumors, human normal colonic epithelium, and human colorectal cancers as described previously (3-6) with a slight modification. In short, tumors or normal epithelia were dissociated by collagenase XI (Sigma) at 37°C for 30 minutes, and the tumor cell aggregates or crypts/glands units were passed through a 100- $\mu$ m cell strainer, centrifuged at 50 *g*, and embedded in Matrigel (BD Biosciences, San Jose, CA). For organoid culture of murine intestinal tumors, advanced DMEM/F-12 (Thermo Fisher Scientific, Waltham, MA) supplemented with 50 ng/mL mouse EGF (PeproTech, Rocky Hill, NJ), penicillin/streptomycin, 10 mmol/L HEPES, GlutaMAX, and 1xB27 (all from Thermo Fisher Scientific) were added to each well. For organoid culture of human colorectal cancers, advanced DMEM/F-12 supplemented with 10% FBS, penicillin/streptomycin, and GlutaMAX were added to each well. For spheroid culture of normal colonic epithelium, 50% conditioned medium of L-cell line secreting Wnt3a, R-spondin3, and Noggin (L-WRN CM) supplemented with 10  $\mu$ mol/L Y-27632 (Tocris Bioscience, Bristol, UK) and 10  $\mu$ mol/L SB431542 (Tocris Bioscience) was added to each well. L-WRN CM was prepared from L-WRN (ATCC; CRL-3276) as described previously (4). According to the experimental scheme, 20 ng/mL

recombinant murine IL-13 (PeproTech), 20 ng/mL recombinant human IL-13, 20 ng/mL recombinant human IL-25, 0.4 µg/mL anti-human IL-25 antibody (R&D), and 0.4 µg/mL normal goat IgG control (all from R&D, Minneapolis, MN) were added to the medium every other day. For cultures of FACS-sorted murine tumor single cells, 10 µmol/L Y-27632 was added to the medium. For *in vitro* induction of Cre-mediated recombination, 1 µmol/L 4-hydroxytamoxifen (4-OHT; Sigma) was added to the medium. In the lineage tracing experiments of murine intestinal tumors, 1 mM valproic acid (Tocris Bioscience) was added to the medium to promote reporter expression (7, 8). For *in vitro* ablation experiments of hCRC organoids, 10 nM dimerizer and 1 µmol/L 4-OHT were added to the medium.

### **CRISPR-Cas9 genome editing of organoids**

CRISPR-Cas9 plasmid targeting the stop codon of IL17RB was generated by cloning 20-bp target sequence into a pX330 plasmid (Addgene #42230).

Homologous arms (approximately 750 bp each) for IL17RB-CreERT2-knock-in were amplified by high-fidelity PCR and cloned into 2A-CreERT2-*frt*-Neo-*frt* cassette to construct the targeting vector. Plasmid constructions were verified

by sequencing. We transfected the CRISPR-Cas9 plasmid and the targeting plasmid to single cell suspensions of human colorectal cancer organoids with Lipofectamine 2000 (Thermo Fisher Scientific) as previously reported (9), and three days after transfection, the organoids were selected with G418 (400-800 µg/mL, Sigma) treatment for 10-14 days. Then, single organoids were picked and expanded, and genotyping for positive clones was performed as illustrated in Supplementary Figure 8. For the excision of Neomycin selection cassette flanked by Frt sequences, we transiently infected FLP- and GFP-expressing adenovirus (Ad-GFP-FLPo, Vector Biolabs, Malvern, PA) to the positive clones. Four days after infection, we sorted single GFP<sup>+</sup> cells from the organoids and cultured them. Then, single organoids were picked and expanded again to select the clones with complete deletion of Neomycin selection cassette by PCR screening. The sequences of sgRNA, PCR screening primers, and the genomic location of homologous arms are listed in Supplementary Table 1.

### **Lentivirus transduction**

For virus production, HEK293T cells were transfected with the pLV-CMV-LoxP-DsRed-LoxP-eGFP (10) (Addgene #65726, a kind gift from Jacco van

Rheenen), pCAG-HIVgp, and pCMV-VSV-G-RSV-Rev (kind gifts from Dr. Hiroyuki Miyoshi, RIKEN BioResource Center, Tsukuba, Japan) plasmids. The culture supernatants were collected 48 h after transfection, filtered, concentrated by ultracentrifuge at 50,000 *g* and re-suspended in HBSS. Single cell suspensions of human colorectal cancer organoids were transduced with lentivirus as previously described (11). After puromycin selection (2-4  $\mu\text{g}/\text{mL}$ ), we sorted DsRed<sup>+</sup> cells to culture organoids with high expression of the reporters. To construct pLV-CMV-LoxP-DsRed-LoxP-iCaspase9-2A-eGFP plasmid, iCaspase9 was amplified from pMSCV-F-del-Casp9-IRES-GFP plasmid (Addgene # 15567, a gift from David Spencer) by high-fidelity PCR and cloned into pLV-CMV-LoxP-DsRed-LoxP-eGFP plasmid using In-Fusion HD cloning kit (Takara).

### **siRNA transfection**

Single cell suspensions of human colorectal cancer organoids were transfected with 10 nM siRNA targeting IL17RB (Thermo Fisher Scientific, Silencer Select siRNA S30959 and S30960) using Lipofectamine RNAiMAX reagent. After

spinoculation at 32°C for 1 h and incubation at 37°C for 4 h, cell suspensions were collected and embedded in Matrigel.

### **Xenotransplantation of organoids**

Human colorectal cancer organoids were dissociated by TrypLE Express (Thermo Fisher Scientific) for 10 min at 37°C and approximately  $1 \times 10^6$  cells were re-suspended in 200  $\mu$ L of culture medium mixed with Matrigel (BD Biosciences) at 1:1 ratio and injected subcutaneously into NOD/SCID mice or nude mice. Tumor volumes were calculated according to the formula (length  $\times$  width<sup>2</sup>) / 2. For orthotopic transplantation, single cell suspensions of human colorectal cancer organoids were injected submucosally into the rectum of NOD/SCID mice as previously described (12, 13).

### **Histological analyses and immunostaining**

For histological analyses, mouse organs or human xenograft tumors were isolated and fixed overnight in 4% paraformaldehyde, embedded in paraffin, and sectioned at a thickness of 5  $\mu$ m. Sections were then deparaffinized, rehydrated, and stained with hematoxylin and eosin (H&E). For

immunohistochemical analyses, sections were incubated with primary antibody overnight at 4°C and washed with PBS. Washed sections were incubated with biotinylated secondary antibody for 1 hour at room temperature. Sections were then incubated with avidin biotin–peroxidase complex (Vector Laboratories), labeled with peroxidase, and colored with diaminobenzidine substrate (Dako, Glostrup, Denmark). For immunofluorescence, sections were incubated with primary antibody overnight at 4°C and washed with PBS. Washed sections were incubated with fluorescence-conjugated secondary antibody (Thermo Fisher Scientific) for 1 hour at room temperature. Dilutions of primary antibody are listed in Supplementary Table 1.

### **Evaluation of tuft cell-like cancer cells in human colorectal cancers**

For the evaluation of tuft cell-like cancer cells in human colorectal cancers, representative primary tumor sections were selected for each case and immunostained for PLCG2. The entire sections were thoroughly inspected for positively stained tumor cells. We judged the hCRCs as tuft cell-like prominent when PLCG<sup>+</sup> cells were detected and as tuft cell-like non-prominent when PLCG<sup>+</sup> cells were not detected in the tumor epithelial cells. In tuft cell-like

prominent hCRCs, the percentage of PLCG2<sup>+</sup> cancer cells was calculated in randomly selected 20 high-power field images and averaged.

### **Time-lapse imaging**

For two-photon excitation microscopy, LCV110-MPE incubator microscope (Olympus) equipped with a 25×/1.05 water-immersion objective lens (XLPLN 25XWMP2; Olympus), and an InSight DeepSee Laser (Spectra Physics, Santa Clara, CA) were used.

### **qRT-PCR**

Total RNA was extracted from tissues or cells using the RNeasy Mini Kit (Qiagen, Valencia, CA) or the NucleoSpin RNA kit (Takara). Single-strand cDNA was synthesized using a ReverTra Ace qPCR RT Master Mix (Toyobo, Osaka, Japan). qRT-PCR was performed using SYBR Green I Master (Roche Applied Science, Basel, Switzerland) and LightCycler 480 (Roche Applied Science). Values are expressed as arbitrary units relative to GAPDH. Primers are listed in Supplementary Table 1.

## **Microarray analysis**

RNA integrity numbers of RNA samples used in microarray analysis were above

6.8. RNA samples were amplified, labeled, and hybridized to SurePrint G3

Mouse GE v2 8×60K Microarray (Agilent Technologies, Santa Clara, CA). The

scanned images were analyzed with Feature Extraction Software 12.0.3.1

(Agilent Technologies) using default parameters to obtain background-

subtracted and spatially de-trended processed signal intensities, which were

normalized by the global scaling method. A trimmed mean probe intensity was

determined by removing 2% of the lower and the higher end of the probe

intensities in order to calculate the scaling factor. Normalized signal intensities

were then calculated from the target intensity on each array using the scaling

factor, so that the trimmed mean target intensity of each array was arbitrarily set

to 2500. Gene set enrichment analysis was performed by GSEA 3.0 software

(Broad Institute). Signal data of overlapping probes were averaged and the heat

map was created by R software (Institute for Statistics and Mathematics).

## **Flow cytometry**

For sorting experiments, tumors were dissociated by collagenase XI for 30 minutes at 37°C and passed through a 100-µm cell strainer, then additionally dissociated with TrypLE Express for 20 minutes at 37°C. Single-cell suspensions were incubated with antibodies for 30 mins at 4°C. For IL17RB staining, PE signal was enhanced by MACS FASER-PE Kit (MACS; Miltenyi Biotech, Bergisch Gladbach, Germany). See Supplementary Table 1 for dilution of antibodies used in this study. Single-cell suspensions were finally passed through a 30-µm cell strainer and sorted by FACSAria II (BD Biosciences). Single cells were gated by forward scatter pulse width and side scatter pulse width. Dead cells were excluded by labeling with 7-AAD. The data were analyzed by using FlowJo software (version 10, TreeStar, Ashland, OR) and FACSDiva software (version 8.0, BD Biosciences).

### **Statistical analysis**

All values are presented as mean ± SEM unless otherwise stated. The two-tailed Student's *t*-test was used for statistical analysis of continuous data.

Fisher's exact test was used for statistical analysis of categorical data. P values of < 0.05 were considered to be significant. Statistical analysis was performed by JMP Pro 13 software (SAS Institute Inc, Cary, NC).

**Data availability**

The microarray dataset in this study is available in the Gene Expression

Omnibus (accession number: GSE 118853).

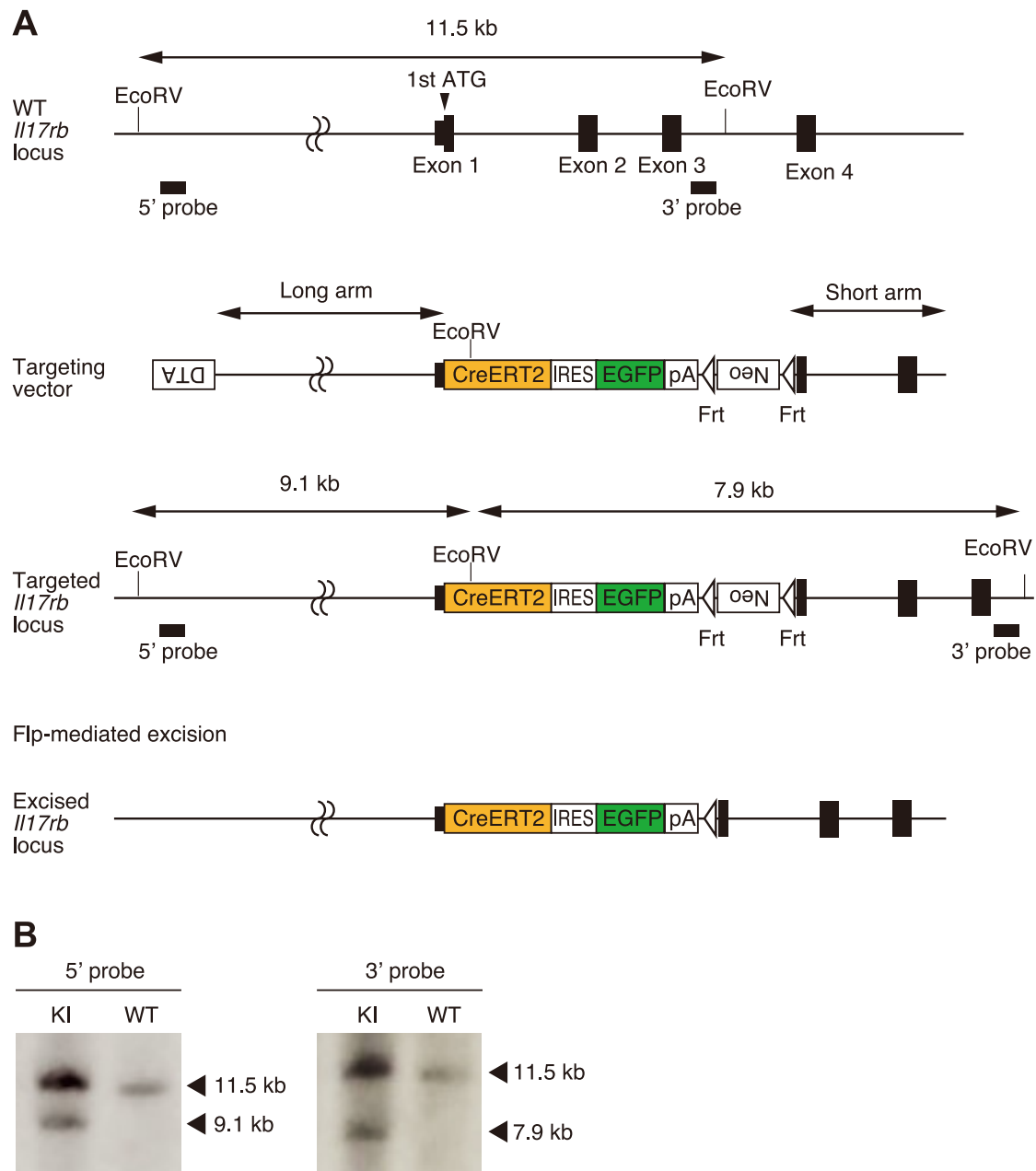


**Fig. S1. Generation of *I117rb-CreERT2-IRES-EGFP* mice.**

(A) CreERT2-IRES-EGFP cassette was cloned into the first ATG codon in exon 1 of the mouse *I117rb* gene. The expression construct was linearized and transfected into C57/BL6 mouse embryonic stem (ES) cells by electroporation and neomycin-resistant recombinant ES clones were selected. All positive clones selected by PCR screening were then confirmed by Southern blotting using the 5' and 3' probes. The neomycin selection cassette was later excised *in vivo* by crossing with CAG-FLP mice.

(B) Representative Southern blotting using the 5' and 3' probes.

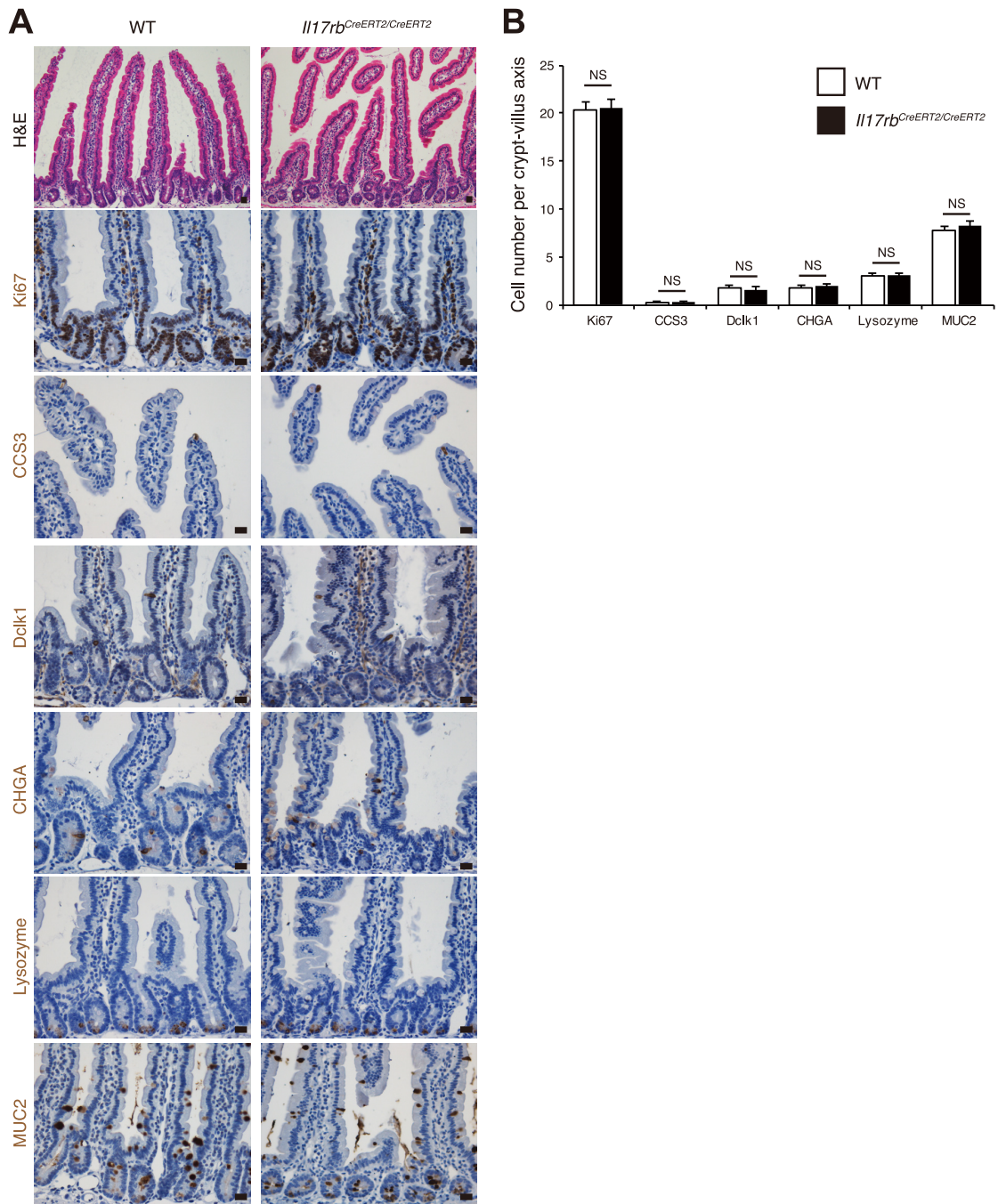


**Fig. S2. *Il17rb<sup>CreERT2/CreERT2</sup>* mice did not show any difference in the intestine compared with wild-type mice.**

(A) H&E staining and immunostaining for Ki67, cleaved caspase-3, Dclk1, Chromogranin A, Lysozyme, and MUC2 in the intestine of wild-type mice and *Il17rb<sup>CreERT2/CreERT2</sup>* mice. Scale bars, 20  $\mu$ m

(B) Quantification of positively stained cells for Ki67, cleaved caspase-3, Dclk1, Chromogranin A, Lysozyme, and MUC2 did not show any difference between wild-type mice and

*Il17rb<sup>CreERT2/CreERT2</sup>* mice.  $n = 20$ . \*,  $P < 0.05$ ; NS, not significant; two-tailed unpaired Student's  $t$ -test. Data are mean  $\pm$  SEM.

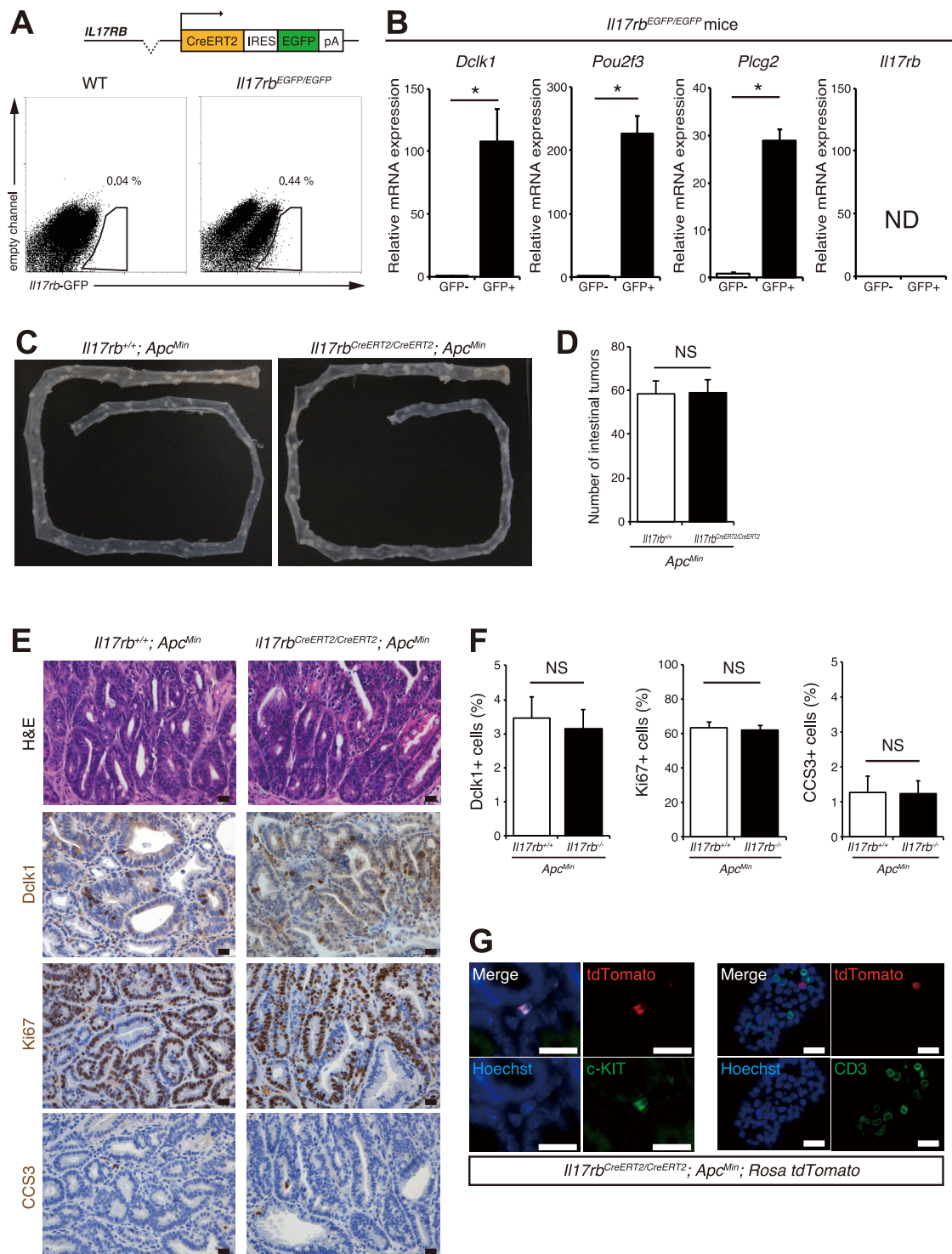


**Fig. S3. *Il17rb* is functionally dispensable for intestinal tumorigenesis.**

(A) Flow cytometry of intestinal epithelial cells of wild-type mice and *Il17rb<sup>CreERT2-IRES-EGFP/CreERT2-IRES-EGFP</sup>* mice.

(B) qRT-PCR of sorted GFP<sup>+</sup> cells from the intestinal epithelium of *Il17rb<sup>CreERT2-IRES-EGFP/CreERT2-IRES-EGFP</sup>* mice showed significant upregulation of *Dclk1*, *Pou2f3*, and *Plcg2* mRNA expression levels and null expression of *Il17rb*. *n* = 3.

(C and D) Macroscopic images (C) and the number of the intestinal tumors (D) in the small intestine of *Il17rb<sup>+/+</sup> Apc<sup>Min</sup>* and *Il17rb<sup>CreERT2/CreERT2</sup>; Apc<sup>Min</sup>* mice. *n* = 7.

(E) H&E staining and immunostaining for Dclk1, Ki67, and cleaved caspase-3 in the intestinal tumors of *Apc<sup>Min</sup>* mice and *Il17rb<sup>CreERT2/CreERT2</sup>; Apc<sup>Min</sup>* mice.

(F) Quantification of positively stained cells for Dclk1, Ki67, and cleaved caspase-3 did not show any difference between the intestinal tumors of *Apc<sup>Min</sup>* mice and *Il17rb<sup>CreERT2/CreERT2</sup>; Apc<sup>Min</sup>* mice. *n* = 10.

(G) tdTomato<sup>+</sup> cells were colocalized with c-Kit<sup>+</sup> cells but not with CD3<sup>+</sup> cells in the intestinal stroma of *Il17rb<sup>CreERT2/CreERT2</sup>; Apc<sup>Min</sup>; Rosa tdTomato* mice after tamoxifen induction.

\*, *P* < 0.05; ND, not detected; NS, not significant; two-tailed unpaired Student's *t*-test. Data are mean ± SEM. Scale bars, 20 μm (E,G).

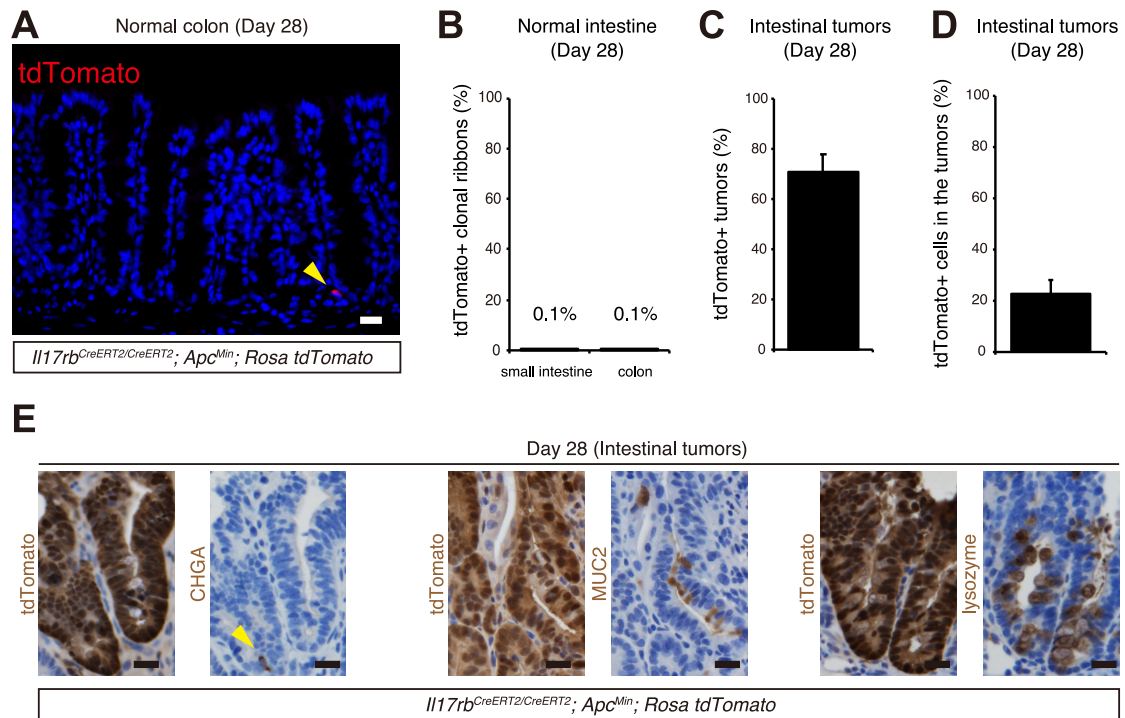


**Fig. S4. Lineage tracing of  $Il17rb^{CreERT2/CreERT2}; Apc^{Min}; Rosa26\ tdTomato$  mice.**

(A) tdTomato<sup>+</sup> cells are only detected in the stroma of the normal colon of  $Il17rb^{CreERT2/CreERT2}; Apc^{Min}; Rosa26\ tdTomato$  mice at day 28 after tamoxifen injection. (B) The percentage of tdTomato<sup>+</sup> clonal ribbons in the normal intestine and in the normal colon of  $Il17rb^{CreERT2/CreERT2}; Apc^{Min}; Rosa26\ tdTomato$  mice at day 28 after tamoxifen injection.  $n = 5$ . (C) The percentage of tdTomato<sup>+</sup> adenomas in  $Il17rb^{CreERT2/CreERT2}; Apc^{Min}; Rosa26\ tdTomato$  mice at day 28 after tamoxifen injection.  $n = 4$ . (D) The percentage of the tdTomato<sup>+</sup> cells within the adenomas in  $Il17rb^{CreERT2/CreERT2}; Apc^{Min}; Rosa26\ tdTomato$  mice at day 28 after tamoxifen injection.  $n = 20$ . (E) Immunostaining for tdTomato and Chromogranin A; tdTomato and MUC2; tdTomato and Lysozyme in the serial sections of the tumors of  $Il17rb^{CreERT2/CreERT2}; Apc^{Min}; Rosa26\ tdTomato$  mice at day 28 after tamoxifen injection.

Data are mean  $\pm$  SEM. Scale bars 20  $\mu$ m (A,E).

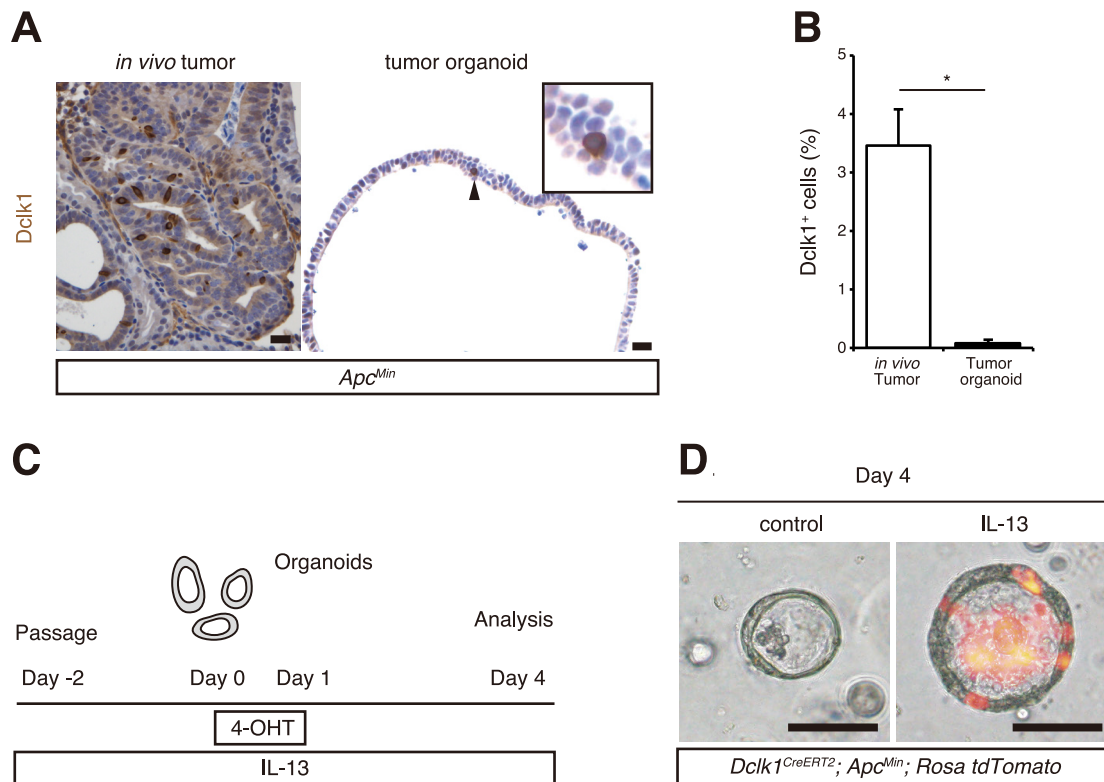


**Fig. S5. Dclk1<sup>+</sup> tumor cells in the mouse adenomas are IL-13 dependent**

(A and B) Immunostaining (A) and the number of Dclk1<sup>+</sup> cells (B) of *in vivo* tumors and tumor organoids of *Apc<sup>Min</sup>* mice.  $n = 10-20$ .

(C and D) Strategy of lineage tracing in *Dclk1<sup>CreERT2</sup>; Apc<sup>Min</sup>; Rosa26 tdTomato* tumor organoids cultured with IL-13 (C) and the representative images of the organoids 4 days after 4-OHT administration (D).

\*,  $P < 0.05$ ; two-tailed unpaired Student's *t*-test. Data are mean  $\pm$  SEM. Scale bars 20  $\mu\text{m}$  (A), 100  $\mu\text{m}$  (D).

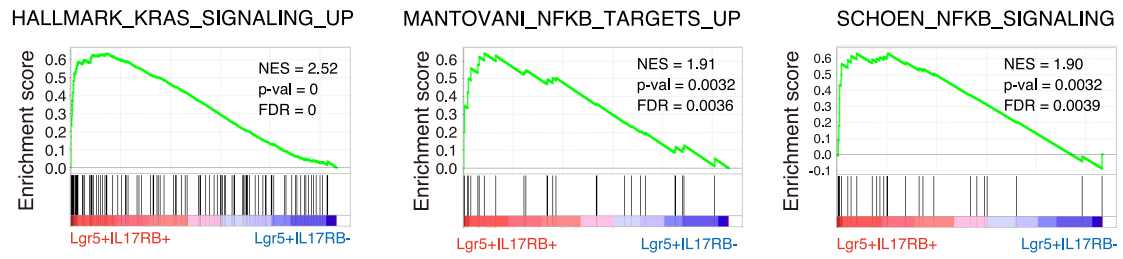


**Fig. S6. Gene Set Enrichment Analysis (GESA) between Lgr5<sup>+</sup>IL17RB<sup>+</sup> and Lgr5<sup>+</sup>IL17RB<sup>-</sup> tumor cells.**

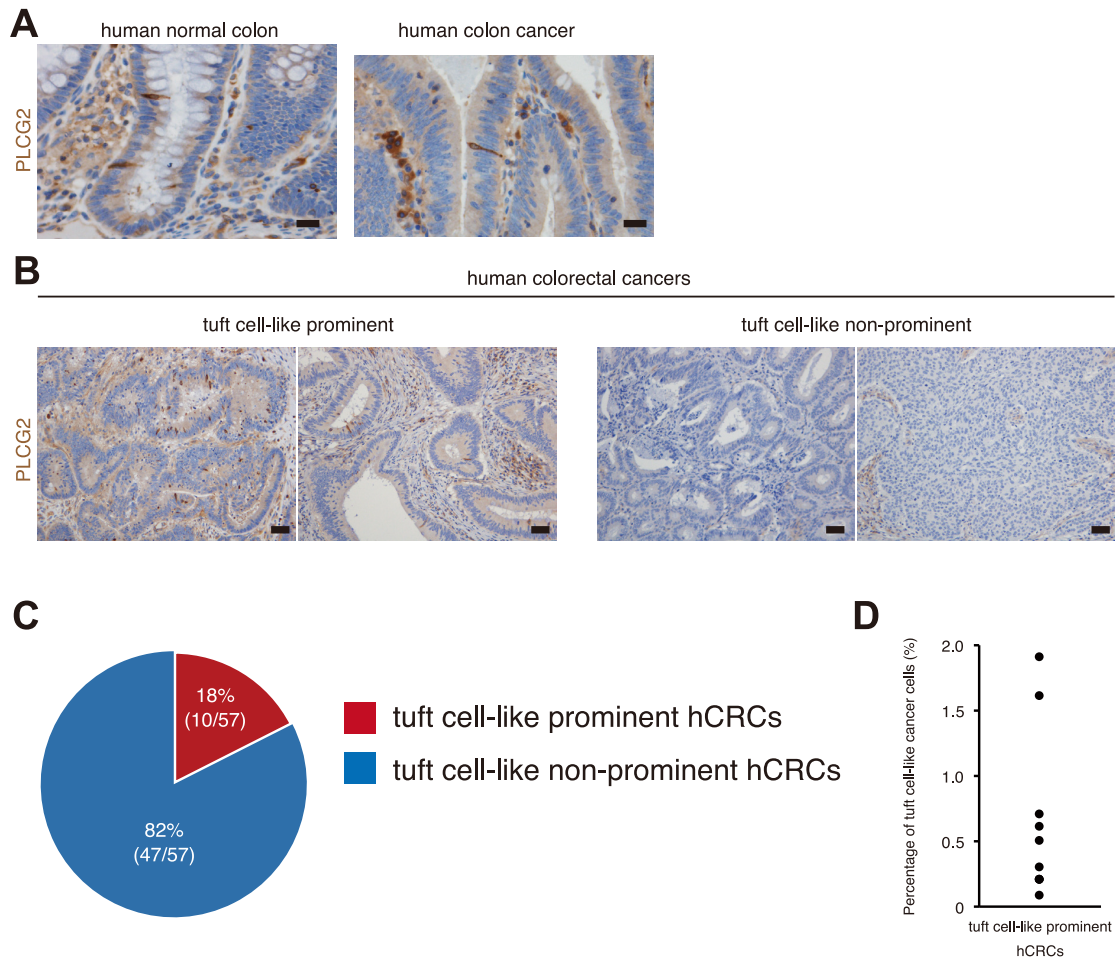


**Fig. S7. Tuft cell-like prominent and non-prominent human colorectal cancers.**

(A) Immunostaining for PLCG2 stably marked tuft cells and tuft cell-like cancer cells in human normal and cancerous colon. Scale bars, 20  $\mu\text{m}$ .

(B) Immunostaining for PLCG2 in human colorectal cancers showed tuft cell-like prominent and non-prominent cases. Scale bars, 50  $\mu\text{m}$ .

(C) Tuft cell-like prominent human colorectal cancers (hCRCs) accounted for 18% (10/57 cases), while tuft cell-like non-prominent hCRCs accounted for 82% (47/57 cases).

(D) Percentage of tuft cell-like cancer cells in the primary tumors of tuft cell-like prominent hCRCs (10 cases). Percentage of tuft cell-like cancer cells in each case was calculated by averaging the percentage of PLCG2<sup>+</sup> cells in randomly selected 20 high-power field images.

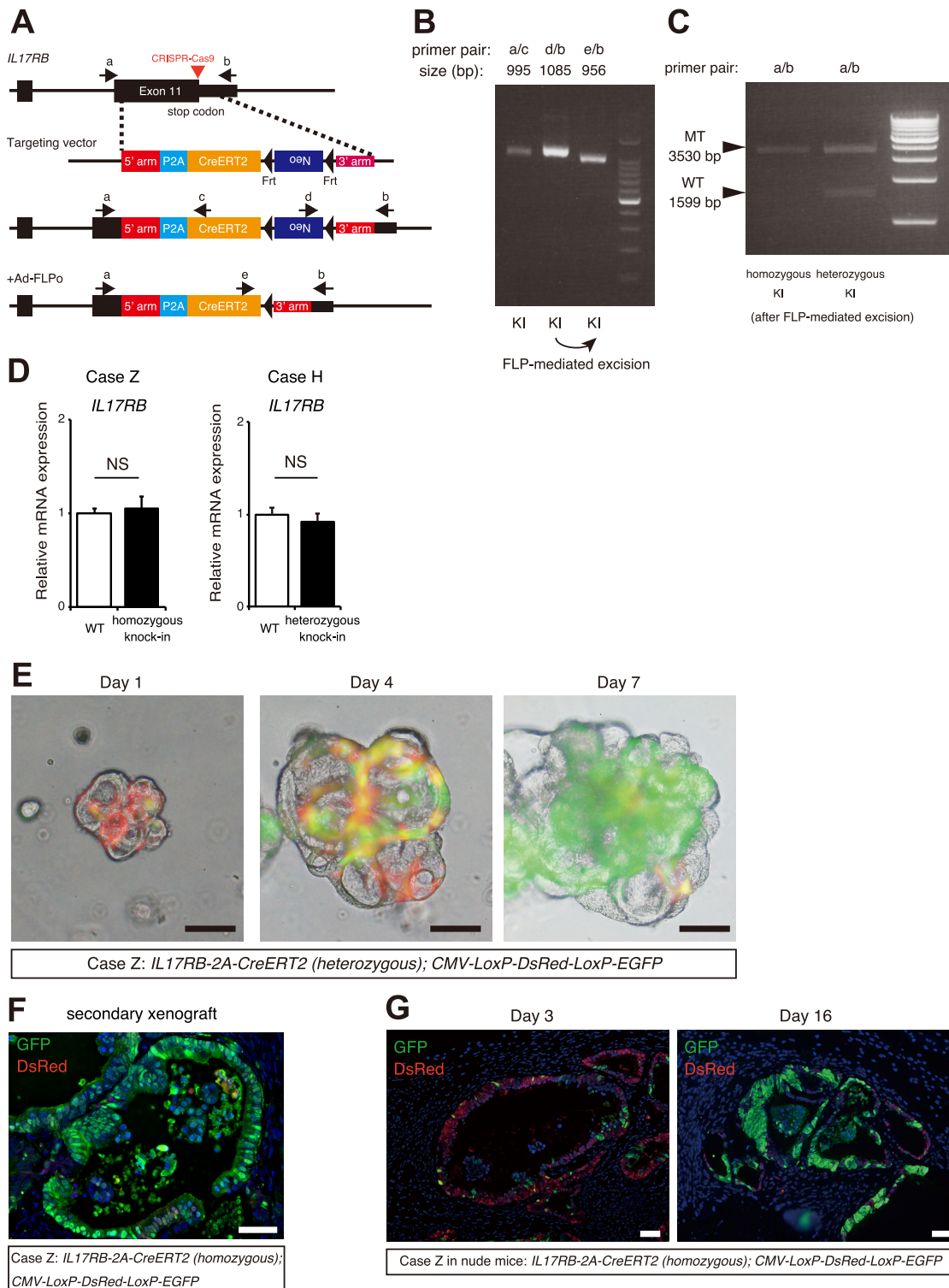


**Fig. S8. Generation of *IL17RB-2A-CreERT2* colorectal cancer organoids.**

(A) CRISPR–Cas9 plasmid targeting the stop codon of *IL17RB* and targeting vector with homologous arms flanking 2A-CreERT2–*frt*–Neo–*frt* cassette were transfected to human colorectal cancer organoids. Neomycin-resistant clones were selected and screened by PCR.

The neomycin selection cassette of the positive clones was later excised by transient infection of FLP-expressing adenovirus. Primer sequences, sgRNA sequence, and genomic location of the homologous arms are listed in Supplementary Table 1.

(B and C) Representative PCR of positive clones before and after excision of the neomycin selection cassette.

(D) qRT-PCR revealed that *IL17RB* mRNA expression levels of the *IL17RB-2A-CreERT2* knock-in organoids are not affected compared with those of the organoids before genome editing.  $n = 3$ .

(E) Time course images of *IL17RB-2A-CreERT2* (*heterozygous*); *CMV-LoxP-DsRed-LoxP-eGFP* human colorectal cancer organoids of case Z after 4-OHT administration.

(F) Persistent expansion of the GFP<sup>+</sup> reporter cells in a secondary xenografted tumors serially transplanted from tamoxifen-treated *IL17RB-2A-CreERT2* (*homozygous*); *CMV-LoxP-DsRed-LoxP-eGFP* xenograft tumors of case Z.

(G) Lineage tracing of xenograft tumors of *IL17RB-2A-CreERT2* (*homozygous*); *CMV-LoxP-DsRed-LoxP-eGFP* human colorectal cancer organoids of case Z transplanted in nude mice subcutaneously. GFP<sup>+</sup> cells at day 3 gave rise to progeny cells and spread to most part of the clones by day 16 after tamoxifen injection.

NS, not significant; two-tailed unpaired Student's *t*-test. Data are mean  $\pm$  SEM. Scale bars 100  $\mu$ m (E), 50  $\mu$ m (F,G).

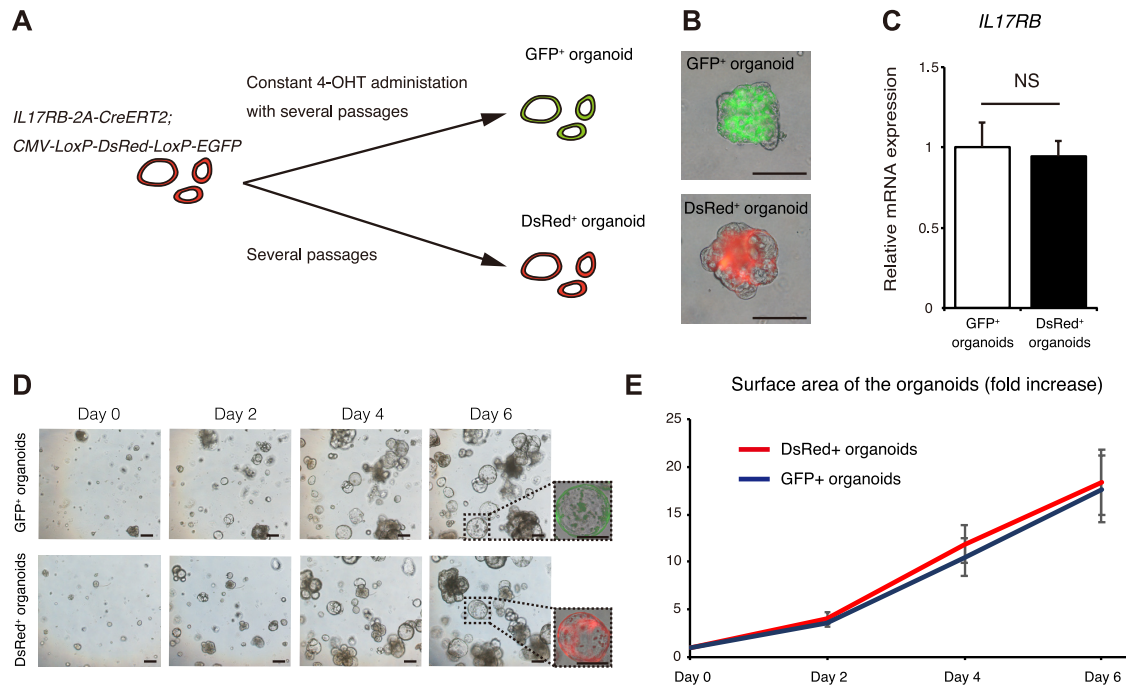


**Fig. S9. Fluorescent color difference does not affect the organoid growth.**

(A and B) Strategy to generate GFP<sup>+</sup> organoids; constant administration of 4-OHT to *IL17RB-2A-CreERT2* (homozygous); *CMV-LoxP-DsRed-LoxP-eGFP* human colorectal cancer organoids of case Z during several passages (A). The representative pictures of GFP<sup>+</sup> organoids and DsRed<sup>+</sup> organoids (B).

(C) qRT-PCR of *IL17RB* in GFP<sup>+</sup> organoids and DsRed<sup>+</sup> organoids.  $n = 3$ .

(D and E) Time course images (D) and the surface areas (E) of the GFP<sup>+</sup> organoids and the DsRed<sup>+</sup> organoids.  $n = 20$ .

NS, not significant; two-tailed unpaired Student's *t*-test. Data are mean  $\pm$  SEM. Scale bars 200  $\mu$ m (B,D).

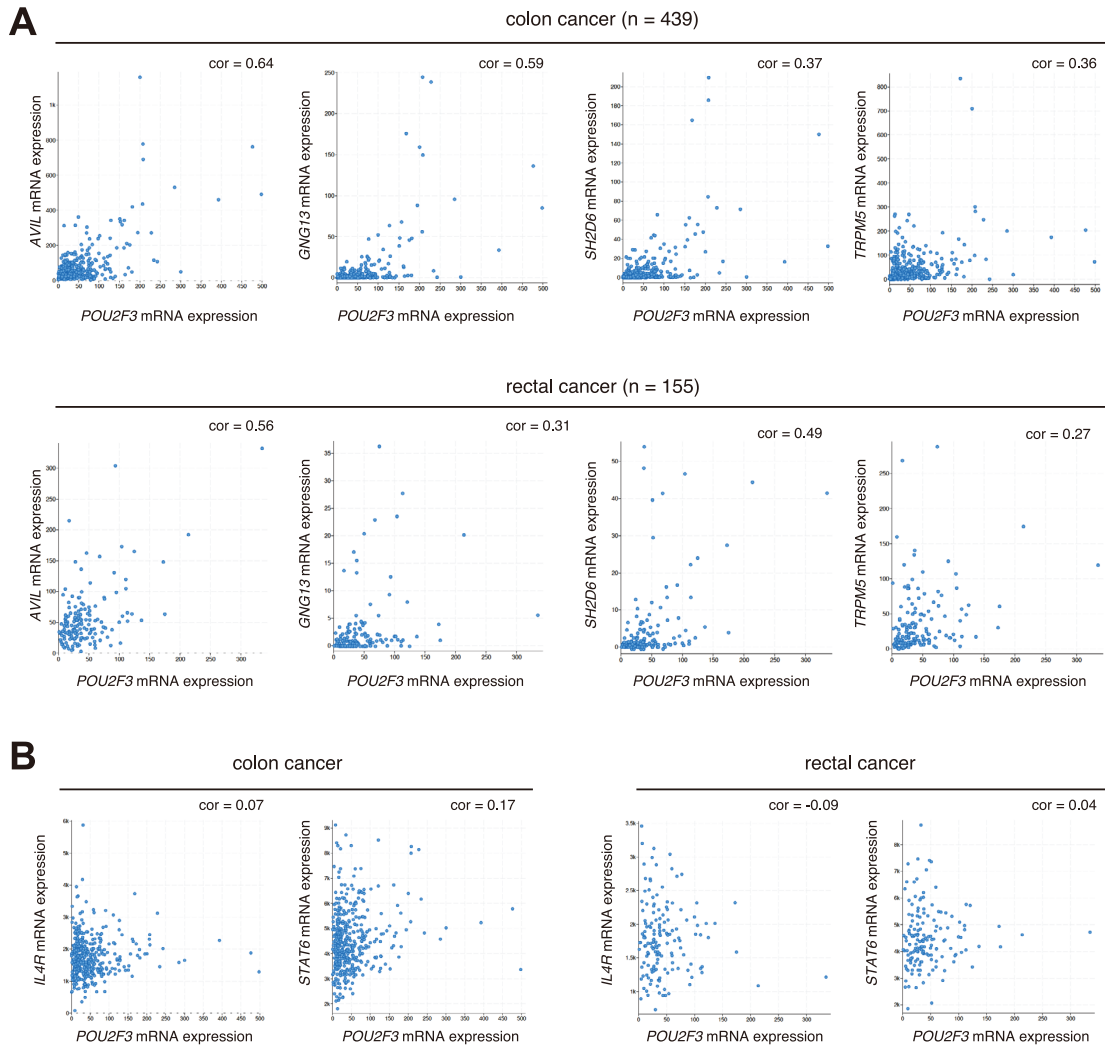


**Fig. S10. *POU2F3* is upregulated in tuft cell-like prominent human colorectal cancers.**

(A and B) Analysis of The Cancer Genome Atlas (TCGA) transcriptome data of colon and rectal cancers revealed that *POU2F3* mRNA expression in both these cancers correlated with expression of tuft cell markers such as *AVIL*, *GNG13*, *SH2D6*, *TRPM5* (A), but did not correlate with *IL4R* or *STAT6* expression (B).  $n = 439$  (colon cancers);  $n = 155$  (rectal cancers). Pearson's correlation coefficients are indicated.

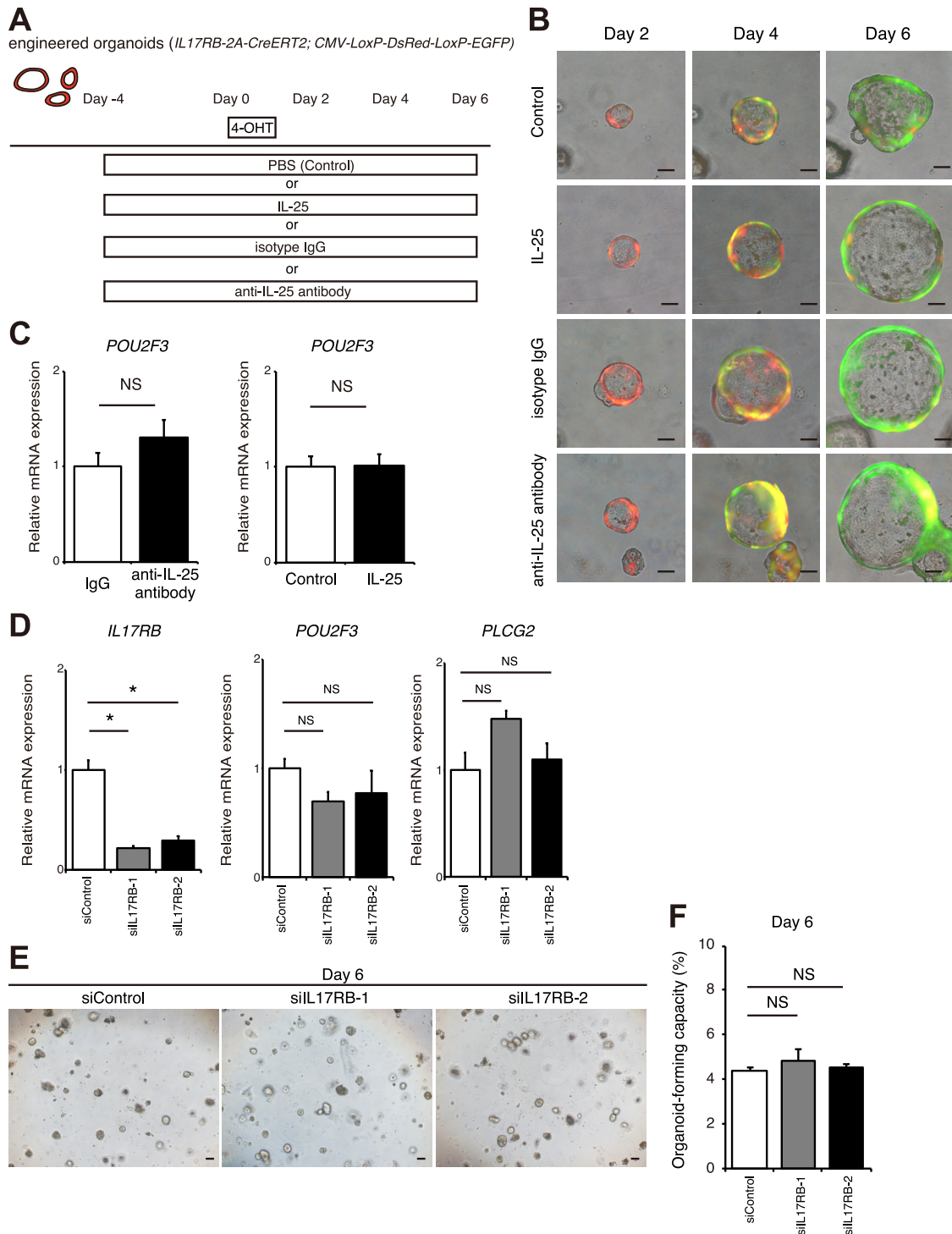


**Fig. S11. The function of IL17RB is not essential for the cell-autonomous expression and self-renewal of IL17RB<sup>+</sup> cancer stem cells.**

(A and B) Strategy (A) and the representative images (B) of the lineage tracing of *IL17RB-2A-CreERT2* (homozygous); *CMV-LoxP-DsRed-LoxP-eGFP* human colorectal cancer organoids of case Z with IL-25 or anti-IL-25 antibody administration.

(C) qRT-PCR revealed that IL-25 or anti-IL25 antibody administration does not affect the *POU2F3* expression levels.

(D) qRT-PCR of *IL17RB*, *POU2F3*, and *PLCG2* in the human colorectal cancer organoids of case H transfected with control siRNA or siIL17RB.  $n = 3$ .

(E and F) The representative images (E) and organoid-forming capacity (F) at day 6 after transfection of control siRNA or siIL17RB to the human colorectal cancer organoids of case H.  $n = 10$ .

\*,  $P < 0.05$ ; NS, not significant; two-tailed unpaired Student's *t*-test. Data are mean  $\pm$  SEM.

Scale bars 100  $\mu\text{m}$  (B,E).

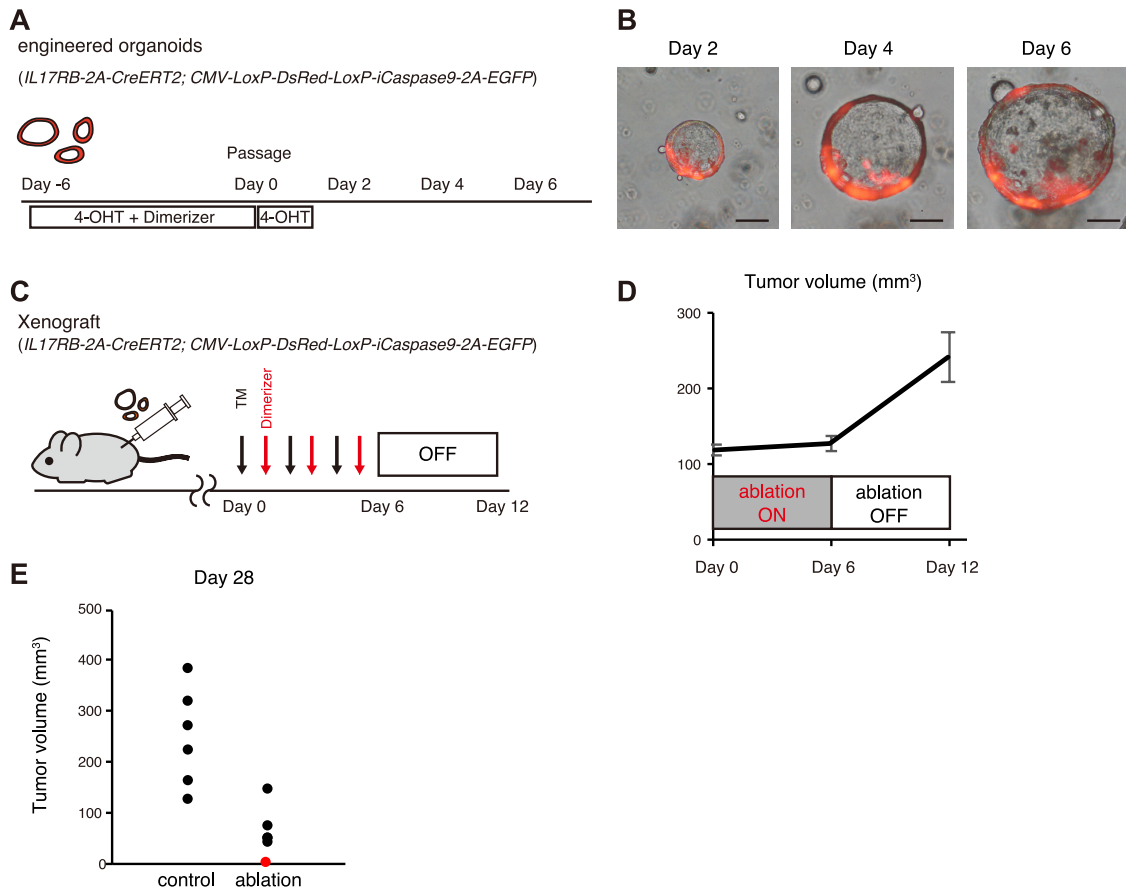


**Fig. S12. Ablation of IL17RB<sup>+</sup> CSCs.**

(A and B) After IL17RB<sup>+</sup> cell ablation, re-administration of 4-OHT does not produce GFP<sup>+</sup> cells in *IL17RB-2A-CreERT2; CMV-LoxP-DsRed-LoxP-iCaspase9-2A-eGFP* hCRC organoids.

(C) Strategy to validate the tumor regrowth after IL17RB<sup>+</sup> cell ablation *in vivo*. Dimerizer and tamoxifen were administered alternately every other days for 6 days and thereafter the treatment was discontinued.

(D) Discontinuation of IL17RB<sup>+</sup> cell ablation resulted in the tumor regrowth.  $n = 4$ .

(E) The volume of each tumor after 28 days of IL17RB<sup>+</sup> cell ablation. The red point indicates one tumor that showed complete regression.  $n = 6$ .

Data are mean  $\pm$  SEM. Scale bars 100  $\mu$ m (B).

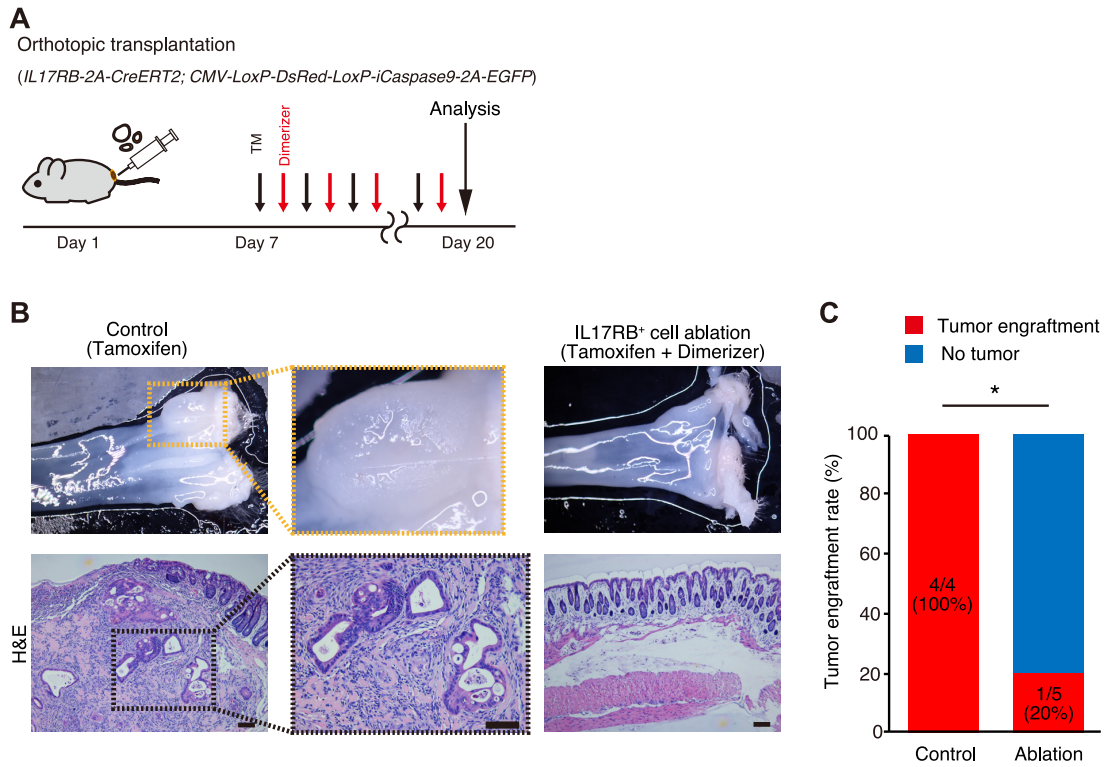


**Fig. S13. Ablation of IL17RB<sup>+</sup> CSCs in the orthotopically transplanted tumors.**

(A) Strategy to evaluate the effect of IL17RB<sup>+</sup> cell ablation in the orthotopically transplanted tumors.

(B) Macroscopic images and H&E staining of the rectum of the control mouse and the IL17RB<sup>+</sup> cell ablation mouse.

(C) Tumor engraftment rate was significantly reduced after IL17RB<sup>+</sup> cell ablation in the orthotopically transplanted tumors.  $n = 4-5$ .

\*,  $P < 0.05$ ; Fisher's exact test. Scale bars 100  $\mu\text{m}$  (B).

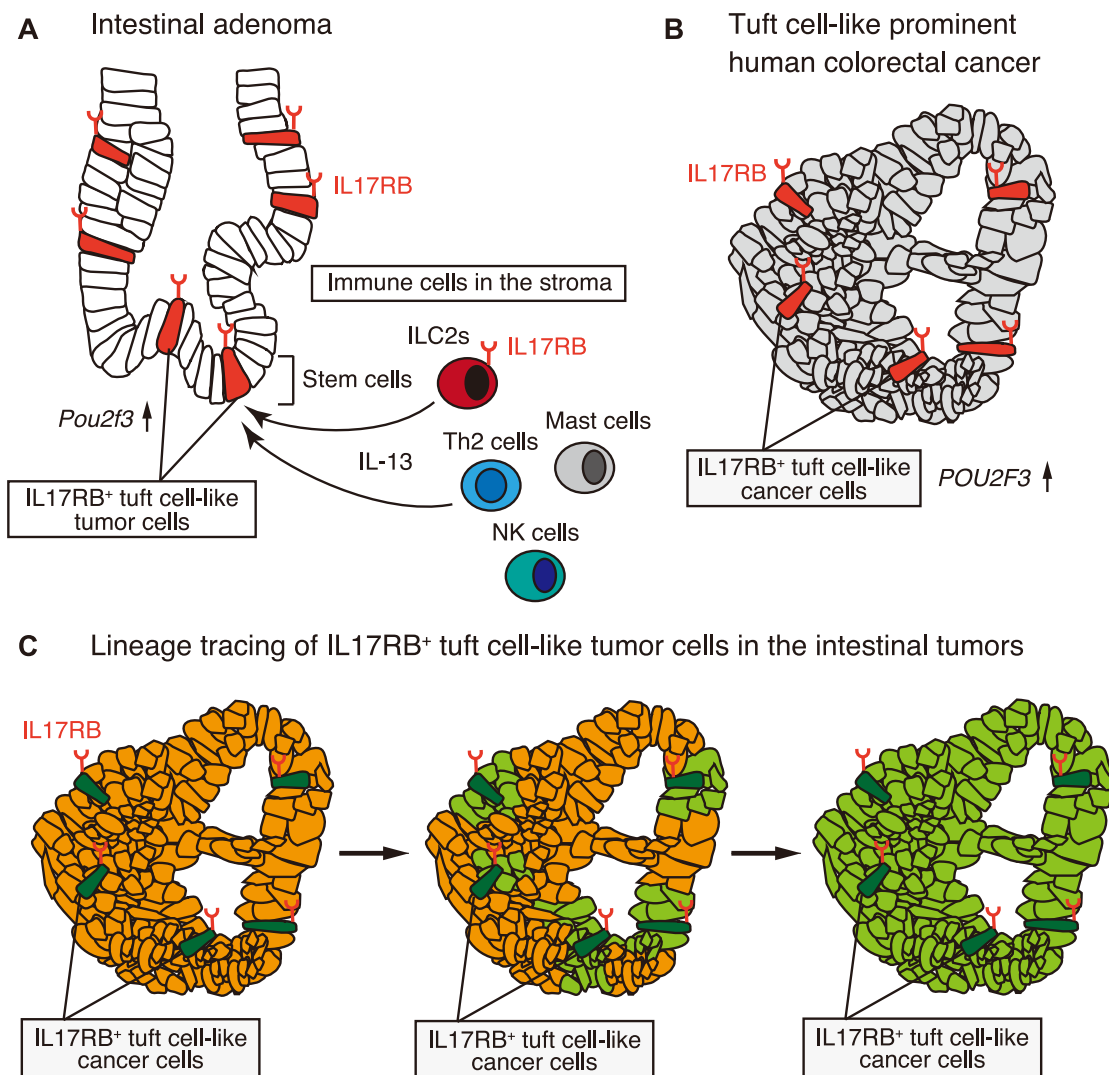


**Fig. S14. IL17RB marks TSCs in mouse intestinal adenomas and CSCs in hCRCs.**

(A) In the mouse intestinal adenoma, IL17RB marks TSCs in an IL13-dependent manner.

(B) In tuft cell-like prominent hCRCs, IL17RB marks hCRC stem cells independently of IL-13.

*POU2F3* expression is upregulated and tuft cell-like differentiation is cancer-epithelial-cell-autonomous.

(C) Lineage tracing of IL17RB<sup>+</sup> tuft cell-like tumor cells in the intestinal tumors.

**Table S1.**

**A** Immunohistochemistry Antibodies

Target	Host	Manufacturer	catalog number	Dilution
CD3	rat	abcam, Cambridge, MA	ab11089	1:250
CD45	rat	BD Biosciences, San Jose, CA	550539	1:20
Chromogranin A	rabbit	Abcam, Cambridge, MA	ab15160	1:100
c-KIT	rat	BD Biosciences, San Jose, CA	553352	1:100
cleaved caspase-3	rabbit	Cell Signaling Technology, Danvers, MA	9664	1:200
Dclk1	goat	Santa Cruz Biotechnology, Santa Cruz, CA	SC-46312	1:100
Dclk1	rabbit	abcam, Cambridge, MA	ab31704	1:200
GFP	goat	abcam, Cambridge, MA	ab6673	1:500
Ki67	mouse	BD Biosciences, San Jose, CA	550609	1:400
Ki67	rabbit	Abcam, Cambridge, MA	ab15580	1:100
Lysozyme	rabbit	Abcam, Cambridge, MA	ab108508	1:1000
MUC2	rabbit	Santa Cruz Biotechnology, Santa Cruz, CA	SC-15334	1:100
PLCG2	rabbit	Santa Cruz Biotechnology, Santa Cruz, CA	SC-407	1:100
PLCG2	mouse	Santa Cruz Biotechnology, Santa Cruz, CA	SC-5283	1:100
POU2F3	rabbit	Atlas antibodies, Bromma, Sweden	HPA019652	1:100
RFP	rabbit	Rockland, Limerick, PA	600-401-379	1:400

**B** Flow Cytometry Antibodies

Target	conjugate	Host	Manufacturer	catalog number	Dilution
EpCAM	eFluor 450	rat	eBioscience, San Diego, CA	48-5791-80	1:50
IL17RB	PE	rat	eBioscience, San Diego, CA	12-7361-80	1:100

**C** qRT-PCR Primers

Species	Target	Forward Primer (5' -> 3')	Reverse Primer (5' -> 3')
mouse	<i>Gapdh</i>	AGGTCGGTGTGAACGGATTTG	TGTAGACCATGTAGTTGAGGTCA
mouse	<i>Il17rb</i>	AGCCGACTATTCAGTGTGGC	GTCTTGACGAGTCCACTTGG
mouse	<i>Dclk1</i>	CGCTCTTGATAAGGAGAGGCA	CCGAGTTCAATCCCGTGGA
mouse	<i>Pou2f3</i>	AGTGGGGATGTCGCTGATTC	TCCTCCGTCTTAATCTGTCTGTT
mouse	<i>Plcg2</i>	GTGGACACCCTCCAGAATATG	ACCTGCCGAGTCTCCATGAT
human	<i>GAPDH</i>	ATGGGGAAGGTGAAGGTCCG	GGGGTCATTGATGGCAACAATA
human	<i>POU2F3</i>	AGTGGGGATGTAGCCGATTC	GCCTGTTGAAATCTAGGCCAT
human	<i>STAT6</i>	GTTCCGCCACTTGCCAAATG	TGGATCTCCCCTACTCGGTG
human	<i>IL4R</i>	CGTGGTCAGTCCGGAATACTA	TGGTGTGAACTGTCAGGTTTC
human	<i>IL17RB</i>	ATGTGCGCTCGTCTGCTAAG	AGCCACATTGAACGGTCCG
human	<i>PLCG2</i>	TCCACCACGGTCAATGTAGAT	CCCTGGGCGGATTTCTTTTAT

**D** human *IL17RB-2A-CreERT2* Knock-in

sgRNA target gene	sequence (5' -> 3')
human <i>IL17RB</i>	CTTCTCATGGGTGGGCTACA
Homologous arm	Genomic location
5' homologous arm	chr3: 53864554-53865305
3' homologous arm	chr3: 53865309-53866065
PCR primers	sequence (5' -> 3')
a ( <i>IL17RB</i> Fw)	GACTATGTCTCCAAAAAAGTTAAG
b ( <i>IL17RB</i> Rv)	GCACCCACCCCTGTTTTT
c ( <i>CreERT2</i> Rv)	GCAAACGGACAGAAGCATTT
d (Neo Fw)	GGGGAACCTTCTGACTAGGG
e ( <i>CreERT2</i> Fw)	ATGCATTCTTGCAAAAGT

**Movie S1. Time-lapse imaging of *IL17RB-2A-CreERT2; CMV-LoxP-DsRed-LoxP-eGFP* hCRC organoids using two-photon excitation incubator microscopy.**

### Supplemental References

1. Nakanishi Y, *et al.* (2013) Dclk1 distinguishes between tumor and normal stem cells in the intestine. *Nat Genet* 45(1):98-103.
2. Harada N, *et al.* (1999) Intestinal polyposis in mice with a dominant stable mutation of the beta-catenin gene. *EMBO J* 18(21):5931-5942.
3. Sato T, *et al.* (2009) Single Lgr5 stem cells build crypt-villus structures in vitro without a mesenchymal niche. *Nature* 459(7244):262-265.
4. Miyoshi H & Stappenbeck TS (2013) In vitro expansion and genetic modification of gastrointestinal stem cells in spheroid culture. *Nature protocols* 8(12):2471-2482.
5. Miyoshi H, *et al.* (2018) An improved method for culturing patient-derived colorectal cancer spheroids. *Oncotarget* 9(31):21950-21964.
6. Sato T, *et al.* (2011) Long-term expansion of epithelial organoids from human colon, adenoma, adenocarcinoma, and Barrett's epithelium. *Gastroenterology* 141(5):1762-1772.
7. Yin X, *et al.* (2014) Niche-independent high-purity cultures of Lgr5+ intestinal stem cells and their progeny. *Nature methods* 11(1):106-112.
8. Fan S, *et al.* (2005) Valproic acid enhances gene expression from viral gene transfer vectors. *J Virol Methods* 125(1):23-33.
9. Schwank G & Clevers H (2016) CRISPR/Cas9-Mediated Genome Editing of Mouse Small Intestinal Organoids. *Methods Mol Biol* 1422:3-11.
10. Zomer A, *et al.* (2015) In Vivo imaging reveals extracellular vesicle-mediated phenocopying of metastatic behavior. *Cell* 161(5):1046-1057.
11. Koo BK, *et al.* (2012) Controlled gene expression in primary Lgr5 organoid cultures. *Nature methods* 9(1):81-83.
12. Sonoshita M, *et al.* (2011) Suppression of colon cancer metastasis by Aes through inhibition of Notch signaling. *Cancer Cell* 19(1):125-137.
13. Inamoto S, *et al.* (2016) Loss of SMAD4 Promotes Colorectal Cancer Progression by Accumulation of Myeloid-Derived Suppressor Cells through the CCL15-CCR1 Chemokine Axis. *Clin Cancer Res* 22(2):492-501.